Development of a Novel Pixelated Time Projection Chamber Detector: Q-Pix

Dissertation by
Kevin Keefe

A DISSERTATION SUBMITTED TO THE GRADUATE DIVISION OF THE UNIVERSITY OF HAWAI‘I AT MĀNOA IN PARITAL FULFILLMENT OF THE REQUIREMENTS FOR THE DEGREE OF
DOCTOR OF PHILOSOPHY
IN
PHYSICS

KE KULANUI O HAWAI‘I MA MĀNOA
Mānoa, Hawai‘i

April 2023
Dissertation Committee:
Kurtis Nishimura

Chairpersons
Jason Kumar, John Learned, Scott Rowland, Peter Sadowski, Gary Varner
Keywords: Field Programmable Gate Array, Time Projection Chamber, Diffusion

Kevin Keefe
ORCID: 0000-0000

ACKNOWLEDGEMENTS

ABSTRACT

The Standard Model (SM) of physics has proven remarkably successful in past decades, yet some measurements such as neutrino oscillations show that this model is still an incomplete description of nature. The hunt for New Physics (NP) continues at higher energies ($>> 1GeV$) with larger detectors ($\approx 10kT$); the data acquired continually hint at Beyond Standard Model (BSM) physics. One such future detector is The Deep Underground Neutrino (DUNE) detector, which has recently begun construction. This 40-kT scale detector requires high precision in both timing ($<< \mu s$) and spatial resolutions ($\approx 1mm$) for vertex reconstruction of interesting neutrino events. DUNE (as any beam detector) is a combination of two detectors, a near-detector (ND) and a far-detector (FD) for long-baseline neutrino oscillation measurements. In order to meet the required timing and spatial resolution the DUNE-FD is a Liquid Argon Time Projection Chamber (LArTPC) design. Recent work has been done to show that LArTPCs can transition from a traditional wire readout to a pixelated readout, and thus further improve vertex reconstruction. This dissertation discusses recent progress and characterizations of a novel implementation of new a pixelated LArTPC readout technology. This novel readout is based on a charge-integrate-reset circuit at the pixel level (Q-Pix). We present the basic pixel-level readout circuit and the implications such an implementation has when applied at DUNE-FD scales. Further, we demonstrate results from the first-prototype implementation based on Q-Pix has been successfully used with solely over-the-counter electronics to acquire new Liquid Argon diffusion measurements. One crucial problem of any pixelated readout is the the ability to handle a large number of unique data channels ($\approx 100k$). To address the scaling problem we developed and tested a modular digital back-end prototype, and implemented it within the first LArTPC prototype. Next, we discuss nominal DUNE-FD APA system level requirements to achieve a projected required sensitivity, remove backgrounds, pixel-level calibration techniques, and possible methods for particle-identification (PID). Simulation results are also performed based on projected background and high-energy neutrino beam-line events. Finally, based on these results of the prototypes and simulation we discuss the nominal digital back-end readout constraints of a fully realized QPix implementation for a DUNE-FD Module.

TABLE OF CONTENTS

LIST OF ILLUSTRATIONS

LIST OF TABLES

Number *Page*

Chapter 1

INTRODUCTION

This chapter outlines and highlights useful background that will be explored in further detail in upcoming chapters as well as provides an outline for the thesis. We begin with an introduction on the standard model, and how both its success and short comings drive larger and more expensive detectors at the intensity frontier. To elucidate the issues at the forefront of the standard model we provide a brief history, with an emphasis on the detectors and experiments which lead to its formulation. Next, we become more specific and discuss DUNE which is an example of a new, large, and expensive detector which aims to push beyond the Standard Model. Finally, we relate the work presented in this dissertation is based on TPCs and how the novel readout design used here is suited for future expansion into larger detectors.

1.1 The State of Things: The Standard Model

In the history of science, it is easily argued that the most successful of all models has been the Standard Model of physics. The Standard Model (SM) was originally developed in mid to late 1970's, and is the model responsible for unifying the weak, strong, and electromagnetic forces together. It has been made remarkable predictions about the existance of elusive neutrinos, and an extensive number of other particles.

In this section we briefly describe the SM and highlight some (certainly not all) key aspects of its formulation understood today. The SM has stood the test of time, despite many known failures and holes in its predictions. Therefore, we hope to elaborate a bit on its status and predictions to help the reader better appreciate the significance of looking for physics beyond the SM.

The basics of the Standard Model

The SM itself dictates what the fundamental constiuents of matter and energy are. As any theory in science its purpose is to explain observed phenomena. In this case, the observed phenomena is simply all particle interactions which involve mass or energy.

The interactions described by the standard model involve the fundamental particle interactions via three of the four known fundamental forces observed in nature: electromagnetic, weak, and strong forces. One of the current failings of the SM is its inability to incorporate a quantum description of

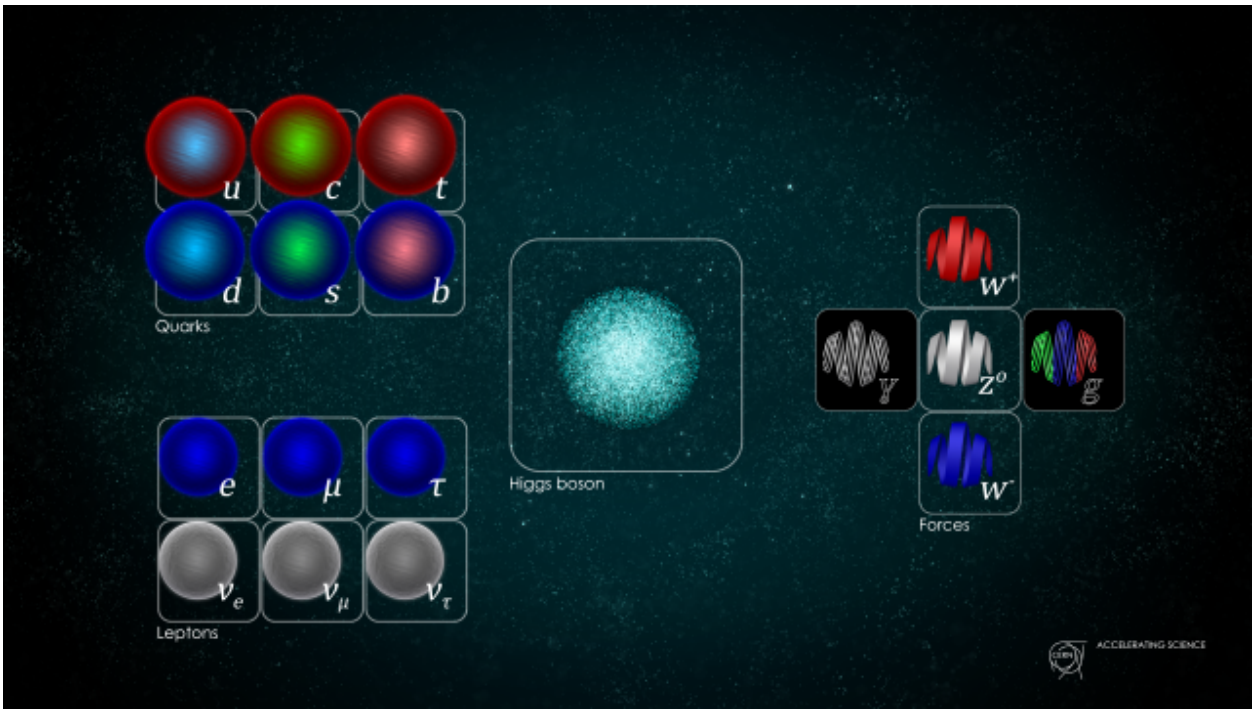

Figure 1.1: Image of Fundamental Particles in the Standard Model, taken from CERN website [1].

gravity. The discussion of the renormalization of quantum-gravity is beyond the scope of the work presented here, and so we only mention that it has to be achieved.

All known fundamental particles are represented in Fig. 1.1.

Quarks

The quarks represent particles in the top left of 1.1. Quarks are the fundamental particles which constitute the "normal" heavy particles, such as protons and neutrons.

Quarks also have unique anti-particles partners of each other. The anti-quark counter-parts have the same mass as the normal partners with all quantum numbers interchanged.

A unique feature of Quarks compared to the leptons is that no "free" Quark has ever been observed. Quarks instead combine either in pairs or in threes to make mesons or baryons, respectively. The mesons contain a quark and an anti-quark, whereas the baryons contain three quarks. Collectively, all particles constituted by any combination of quarks are known as hadrons.

Since quarks are not freely observable a common place to infer their existence (and to create heavier hadrons) are in particle accelerators. The most well known particle accelerator is the Large Hadron Collider (LHC) in Geneva. These Particle accelerators generate extremely high energy ($\approx \mathcal{O}10TeV$) protons which when collided can generate new compositie hadrons of any mass so that the total energy is conserved.

Leptons

The leptons represent particles in the bottom left of 1.1.

The first lepton discovered, and the most easily recognized, is the electron. Just like the quarks, the leptons come in three families (electron, μ, τ). Also like the quarks, the leptons have charge, mass, and flavour which means they can decay.

Unlike the quarks the leptonic particles do not have a color quantum number and therefore do not combine together to create compositive particles. Additionally, free leptons are observed, e.g. the electron.

The most difficult to measure particles of all in the SM are the neutrinos. This is because these leptons carry no net charge. However, since they carry flavour and can decay (or be absorbed) and they also carry their respective lepton number, the neutrinos in the family can be identified by measuring their partner.

For example, a common process to observe an anti-electron neutrino ($\hat{\nu_e}$) is through inverse beta-decay (IBD) following the reaction:

$$\hat{\nu_e} + p \rightarrow e^+ + n \tag{1.1}$$

This IBD reaction is a common measurement tool for identifying neutrinos because of the distinguisable detection signature of the produced particles. The position (e^+) annailates very quickly ($< \mathcal{O}ns$) and will produce back-to-back 511 keV photons. The produced neutron, on the other hand, wobbles around much longer ($\mathcal{O}us$) before being captured, which produces scintillation light of energy proportional to the neutrons energy when captured.

Forces

All forces within the standard model (electromagnetism, weak, and strong) interact via a "carrier" particle. These carrier particles are represented on the center-right of 1.1.

The electromagnetic force is governed by particle exchanges of a photon. Other than perhaps gravity, which isn't explained by the SM, this is the most well known and described force. All particles which carry charge interfact with this force, therefore the neutrinos are the only particles within the quarks and leptons which do not interact at all with the electromagnetic force (this is why detecting them is so hard). The full theoretical description of this force is governed by Quantum-Electrodynamics (QED).

The weak-nuclear force is goverened by particles exchanges of one of the three particles in the center: $W^{\pm}$ and Z. This force involves a change in flavor of a particle, and involves both quarks and leptons. It is also responsible for all decay processes. The theoretical description of these mechanics are called Quantum-Flavourdynamics (QFD).

The strong-nuclear force is goverened by the exchange of the gluon (g). This force is responsible for color changes of matter and describes why nuclei are held together. Since this force only involves exchanges of a gluon, the leptons are therefore unaffected since these particles carry no color quantum number. The full theoretical description for the strong-nuclear force is Quantum-Chromodynamics (QCD).

Higgs

The last particle to be discovered in the SM was the Higgs particle. The Higgs particle was originally predicted in 1964 by Peter Higgs **??**. This particle is important to describe how mass is given the the elementary particles described by the SM. Finally, in 2012 the Large Hadron Collider (LHC) was able to infer the massive higgs particle **??**.

The Frontiers of the Standard Model

Yet, despite its numerous achievements in predictive power and experimental verification we know today that it has crucial shortcomings. The Standard Model (SM) has no ability to account for Dark Matter or Dark Energy in the universe, nor the distribution (or the hierarchy) of neutrino masses, nor is it able to relate how gravity interacts with the other fundamental forces of nature (Unification). It also doesn't account for some 'basic' properties it has, such as: why are there only three generations of laptonic particles (electron, muon, and tau)? These short-comings offer hints for where to search for physics. Physicists have known about these short comings from the conception of the Standard Model and have (to no avail) sought out what's next.

With a plethora of hints to search for NP, it can be useful to organize the efforts of search. In 2008 the p5 committee did just this and labeled the three frontiers of physics as the cosmological, energy,

and intensity frontiers. Each of these frontiers offer different kinds of challenges and aim to search at the

The cosmological frontier aims to search for NP on extremely large time and distance scales by relying on observational techniques. Cosmological measurements have shown the that majority of the universe's matter is not visible to light, and so we call it dark matter. Additionally, the unverise is expanding at an accelerated rate, which we can tell from the blueshift of distance galaxies. Likewise, cosmologists have also discovered that the universe is expanding due to some invisible energy in the universe, and so we call it dark energy. The search for these dark causes of the universe lie within the realm of the cosmological frontier.

The energy frontier is concerned with the origin of mass. The Large-Hadron Collider experiment is the archetypal experiment aimed at solving problems within this frontier.

The third (and final) frontier to mention is the Intensity frontier. The Intensity Frontier of Physics ([5]) is one which requires very large and very precise measurements to gain the statistics to declare an observation. In order to address the issues posed within this frontier the large scale detectors hunting for New Physics (NP) have continued to grow in size, energy sensitivity, and importantly cost: [6].

1.2 How we got here.

Many times since the early 20th century it was thought that the goal of physics was accomplished. However, during each of these moments of false triumph some new detector was built to take a new measurement; thus, the door to new understanding of nature is never closed. This section provides a brief and (necessarily) incomplete history of significant measurements and detector developments relevant to particle physics in the creation of the SM. In order to clear an obstacle, it is often helpful to remember the previous ones.

A Century of New Physics

At the turn of the 20th century particle physics was in its infancy. In 1900 Max Planck first introduces the concept of energy quanta for the first time concerning photons to eliminate the infamous ultra-violet catastrophe problem introduced by statistical mechanics. JJ Thomson used a single cathode-ray tube to discover the electron and the nucleus, and won for himself the Nobel Pize in 1906. Milikan's famous oil-drop experiment won him the Nobel Prize in 1923.

However, as each of these new discoveries solved problems only more questions were produced. Once the nucleus was discovered to contain only protons and neutrons, the natural question arose:

what holds all of the positive charge together in the center. Thus, physicists cleverly named the new force which was stronger than the electromagnetic force: the Strong Force.

The bubble chamber was then invented in 1952 by Donald Glaser [7]. These detectors proved significant in the discover of the W and Z bosons and ultimately allowed the unification of the electromagnetic and weak forces to form the electroweak theory.

Next the spark chamber eventually lead to the gradual development of the wire-spark chamber. In 1968 Georges Charpak developed the Multi-Wire Proportional Chamber (MWPC) for which he (much later) won the Nobel Prize in 1992. From this key insight a new detector concept was made possible.

An Escape: Catch the Neutrino

More than 100 years ago Chadwick was able to show that the energy sprectrum from a decaying electron was continuous [8]. This prompted Wolfgang Pauli to predict a particle which he origianlly called the neutron to also be a decay product, but not easily observable. Quickly however the particle name neutron was taken by a different neutral particle in 1932 [9]

The discovery of the neutron and the continuous spectrum of beta decay caused Pauli to come up with a new theory attempting to describe it [10].

This even lead some physicists to belief that perhaps the conservation of energy was violated. However, the motivation to save this conservation law lead Wolfgang Pauli to the first prediction (1930) of the neutrino; the reason that the energy was a spectrum from the electron was that some of the energy was "taken up" by the neutrino. Finally, some 26 years later in 1956 was the first observation of the electron neutrino [11].

A few years later the first reactor neutrino (ν_μ) was observed at Brookhaven National Laboratory (BNL) [**PhysRevLett.9.36**].

The first measurement of the τ neutrino (ν_τ) happened much later in 2001 [**donut_first_tau_n_measure**]. this detector used nuclear emulsions.

After this first discovery is when the the answers, and mostly the questions started to pile in. Since then, many large-scale experiments have been dedicated to measuring the three generations of neutrinos **??**

Originally the mass of the neutrino predicted by the SM was massless. That was until the Solar-neutrino anomaly measured significantly less neutrinos than predicted **??**. The solution for this was oscillation.

Neutrino Oscillation

Tokai to Kamioka (T2k) [12] has well established neutrino oscillation measurements.

Daya bay [13] has also established measurements of electron anti-neutrino ($\bar{\nu_e}$) disappearance.

Of all known particles the most elusive (hardest to detect and measure) is the neutrino. For this reason the least is known about the neutrino. What we do know about the neutrino is there are three pairs of them, associated with their leptonic partners: the electron, muon, and tau.

It came as a welcome shock that neutrino oscillation was first measured. This oscillation indicates that a neutrino as it moves through space can change its state; a electron neutrino can oscillate into a muon neutrino or even a tau neutrino. This happens because the mass eigenstate and flavor eigenstates which govern the neutrino are not equal.

$$\begin{pmatrix} \nu_e \\ \nu_\mu \\ \nu_\tau \end{pmatrix} = \begin{pmatrix} U_{e1}, U_{e2}, U_{e3} \\ U_{u1}, U_{u2}, U_{u3} \\ U_{\tau 1}, U_{\tau 2}, U_{\tau 3} \end{pmatrix} \begin{pmatrix} \nu_1 \\ \nu_2 \\ \nu_3 \end{pmatrix} \tag{1.2}$$

1.3 Modern Tracking Detectors

It is could said that any definition defining a "new" age of a types of detectors is subjective. Nevertheless, we proceed to define that modern particle detectors were the age that began to use modern electronics based on metal–oxide–semiconductor field-effect transistor (MOS-FET). If there was any invention which was able to drive the development of computers and measuring electronics, it was the transistor.

Therefore, the beginning of the modern particle detection age began with the transistor, and it saw to the end of the spark chamber and bubble chamber detectors.

Multi-Wire Proportional Chamber

The middle of the 20th century saw a dramatic increase in the ability and reduction of the cost of electronics. These (then) new electronics allowed for fast digitizing measurements of voltage or current. Thus, new propotional counter detectors were capable of using computers to do the measuring or counting of the events within the detector. The rate at particles could then be detected increased by orders of magnitude.

Using the fast digitizers and closely spaced wires Georges Charpak (1924-2010) created the first-Wire MWPC in 1968 [14]. This new detector was one which paved the way for modern detector

development, for which Charpak won the 1992 Nobel Prize.

Time Projection Chambers

Time Projection Chambers (TPC) [15] have been shown to be extremely useful in high energy physics experiments due, in part, to their high resolution in both timing and spatial dimensions. This detector was originally used in the Position-Electron Project PEP-4 experiment which measured electron-positron collisions from the 29 GeV electron beam produced at the Stanford Linear Accelerator (SLAC). The first TPC design used high pressure gas and was able to measure 1000s of particle tracks per second (compared to 1-10) and provide full 3-D event reconstruction.

It did not take long for other experimentalists to generalize this concept to different elements or even to liquid.

Noble Gases and Time Projection Chambers

The technology of TPCs has greatly matured since their original inception. in many kinds of detectors across HEP. TPCs can also incorporate two phases of a substance (liquid and gas), called Dual Phase (DP) TPCs.

the Xenon-1T is a dark matter experiment which is a dual-phase TPC [**Aprile_2017_xenon1T**].

The LUX experiment is a single phase TPC also hunting for dark matter.

A specific kind of TCP is a Liquid Argon Time Projection Chamber (LArTPC) [16].

recent work on LArTPCs ([17], [18], [19]).

Energy resolution of the LArTPCs within DUNE are still unknown to within a factor of 4 [20].

The Deep Underground Neutrino Experiment

The Deep Underground Neutrino Experiment (DUNE) is a long-baseline neutrino beam experiment [4, 21–23]. DUNE is composed two detectors, a near (ND) and a far (FD) which are separated by a distance of 1300 km. The ND is located at Fermilab and its purpose is to characterize the source neutrino beam created there. The FD is composed of four separate 10 kiloton modules, all of which will be a single-phase (SP) LArTPC based detector. Two of these four modules at least will use a known wire-based readout technology and a vertical drift-readout. The two remaining modules are considered modules of opportunity and their readout technology is yet unknown. A purpose of this dissertation is show the viability of a novel readout technology.

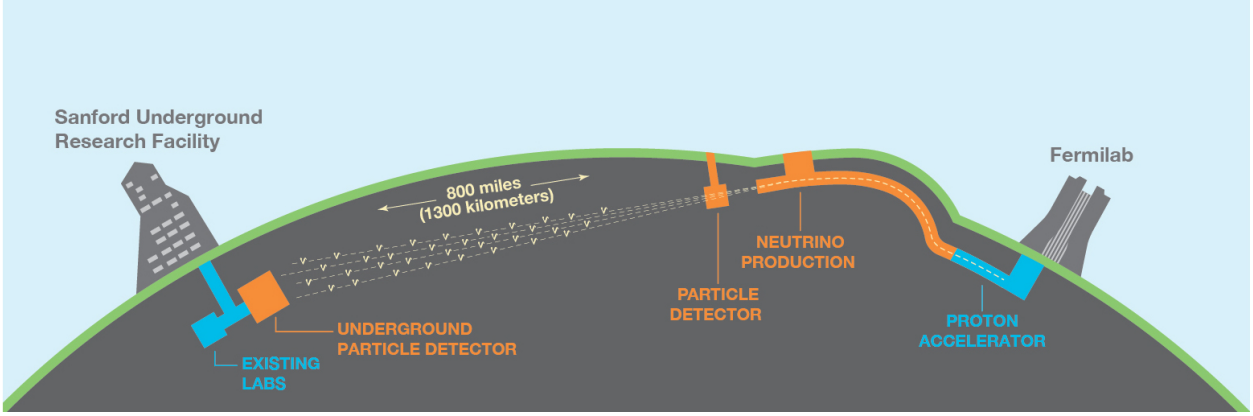

Figure 1.2: Simple Draw up of DUNE FD taken from [2]

DUNE has three main science goals, all of which are geared towards pushing beyond the standard model:

- Hadron Decay
- Neutrinos from Core-collapse supernovae
- Beamline neutrino interactions.

We will discuss the relevance of each of these items, and in 2 we will further discuss how the work presented here relates to each of these topics.

Conventional horizontal drift detection for foreseeable DUNE modules are already considered possible for lengths up to 6.5m [24].

Hadron Decay

Second generation proton decay studies in the ICARUS experiment: [25].

Supernova Studies

The principal decay chain follows the pattern:

$$\nu_e + {}^{40}Ar \rightarrow e^- + {}^{40}Kr^* \tag{1.3}$$

Pixelated Tracking Detectors

1.4 Even Further: Detectors in the Current Century

Finally, in this last section we discuss recent development of various detector technologies. There are many motivating pressures for new detectors to adopt pixelated designs. Below we discuss two contributing factors: the development of electronics and computing algorithms.

First, previously pixelated detectors have historically been more difficult because of the issues of cost and size regarding the number of readout channels. This is being addressed, in part, by the advent of newer, cheaper, and larger Field-Programmable-Gate Arrays (FPGAs). One method for reducing the electronic overhead required in pixelated detectors is to use digital multiplexing. Cheap, high channel FPGAs directly solve this problem. Other electronics development, such as the Silicon-Photomultiplier, offer much cheaper alternatives for large pixel counters compared to their historical counter-parts.

[26] Another driving factor is the the development of Machine Learning (ML) algorithms, particularly Convectional Neural Network (CNN [27]). Recent industry has driven the need for CNNs to be able to correctly identify and label 2-D images of various kinds, and thus championed much of progress in this field and spawned many kinds of CNN algorithms. Recently, it has been shown how these kinds of algorithms extend into High Energy Physics (HEP) for particle identification. A major issue at the Intensity Frontier of physics is the sheer amount of data to store and process. These ML algorithms provied a developed tool to automate the analysis of huge amounts of data ($>> 1TB$) and have been shown to be quite accurate ($> 99\%$) at particle identification in LArTPCs.

Current Pixelization Efforts in TPCs

Additional work has been performed in recent years which show that LArTPCs can also utilized a pixel-based readout [28], [29].

SANDD

Another Example of a pixelated detector is [30].

The Single Volume Scatter Camera

This work is presented in greater detail in (Appendicies-A/B) and represents a substantial amount of my own individual contribution. I am the 2nd author on the the paper described in Appendix-A and the corresponding author of Appendix-B, where I also collected and analyzed all presented data therein.

Future Detectors

The end of the Standard Model era is inevitable. SM simply fails to account for physics with all major frontiers for physicists to accept its completeness; we know there is much and more to learn about nature.

The 20th century saw unprecented progress in its sophistication of its detectors from ray tubes, to spark chambers, to proportional counters, and to huge (>20 km) particle accelerators. This century shows no signs holding any less promise than its predecessor. Continued development in electronics, computing, and analysis methods will lead to more and newer frontiers of physics.

The work presented in this introduction aims to not only encapsulate the massive progress particle physics has made since the electron's discovery, but also to server as a reminder of how extraordinally surprising nature is. At every turn and at every point where physicists think they've arrived at the end (or at an impossible roadblock) there always remains more to discover. If we have learned anything, we have learned to knock and the door shall be opened.

Chapter 2

A NOVEL READOUT TECHNIQUE FOR TPCS: Q-PIX

In this chapter we introduce a novel pixel-based readout technology for TPCs. Pixel based readouts offer several advantages over the traditional wire readout [31]. A key improvement offered is true 3-D image reconstruction. This allows for sharper vertex reconstruction, thereby improving the overall resolution of DUNE and decreasing the required time for a NP measurement. Other advantages are ease of data analysis and reduction in total data storage. A pixel based readout automatically records two of the three spatial dimensions, and thereby provides for simpler analysis. Additionally, the pixelated readout method presented here cuts the total required data storage and data acquisition rate (without loss to precision) by several orders of magnitude.

However, the advantages also come with the cost of increased design complexity as the number of readout channels increases by more than three orders of magnitude. The traditional wire based readout within a DUNE module will include hundreds to thousands of channels, whereas a full DUNE module with a pixel-based readout will have 10's of millions of channels. This number of required channels to be stably readout during DUNE's expected lifetime (> 10 years), where the electronics continually operate at liquid argon temperatures is likely the largest hurtle for a pixel-based design. The aim of this dissertation is to address the channel-size problem.

2.1 Q-Pix: The Circuit Level Design

The fundamental readout circuit (2.1) was first introduced by Nygren and Mei [3]. The principle of the front-end circuit operates on measuring the output of a schmitt trigger whose comparator voltage input is connected to an integrating capacitor circuit.

The circuit input is connected to the anode of a TPC where drifted electron charge accumulates. Voltage is then built up from the charge stored on the pixel based on the capacitance according to the equation:

$$Q_i = C_i V_i \tag{2.1}$$

After the capacitor voltage (V_i) exceeds a set threshold value the schmitt trigger activates. The time

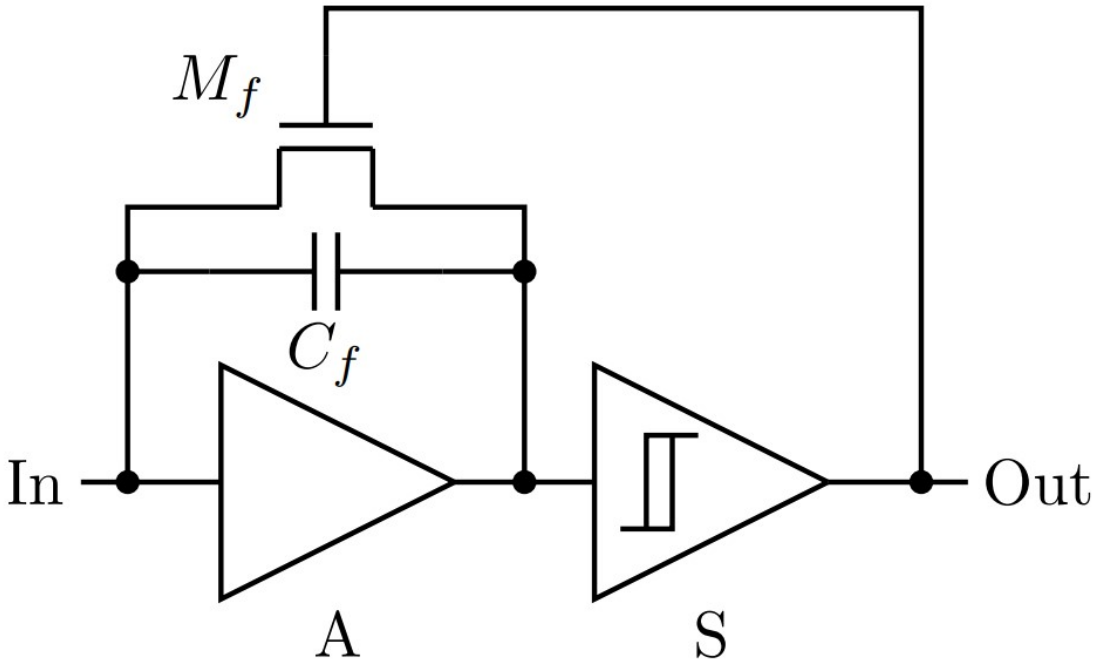

Figure 2.1: Image of Basic Q-Pix Readout circuit. Currently this front-end circuit is being designed as custom analog ASIC which has 16 channels. Image is taken from [3].

of the trigger output is recorded by a digital logic which encodes this data as a 32 bit value. Since the capacitor reset happens at the same time as the issued trigger the digitally-recorded value is the reset time.

We consider that the digital blocks responsible for digitizing the reset to have a nominal frequency of $\approx 30MHz$. Therefore, the minimum time before the recorded time value on each digital clock is calculated by

$$T_{loop} = \frac{2^{32}}{30 * 10^6} \approx 143 seconds \tag{2.2}$$

This time (T_{loop}) indicates the minimum reset time to occur within each responsible digital block.g; Since this time is much greater than the antipcated reset rates to be produced from backgrounds, discussed in a later section 2.1, we expect the looping of the 32-bit recorded value to not be a problem.

Reconstructing Voltage from Time Resets

Here we describe the basic principle of reconstructing the input current from a collection of reset measurements. The key insight for this readout technology is that time (instead of voltage as in a MWPC) is recorded. Therefore, measurements only taken place when there is enough charge to cause a reset which prevents continuous measurements during periods of long dead time. This concept follows the detector concept of least action in that all measurements are detector responses.

A measurement of a reset indicates that a certain amount of charge was discharged from the integrating capacitor. Since total charge is conserved, we can say that the total amount of charge that accumulates onto the pixel is equal to total amount of charge discharged from each reset, plus any residual charge still on the pixel. Therefore, we can relate the total accumulated charge to the total charge discharged with the following equation:

$$Q_{in}(t) = Q_{out}(t) + Q_c(t) \tag{2.3}$$

eq:qin)

If we assume that each reset removes the same amount of charge during each reset then we can rewrite Q_{out} in terms of N_t where N_t is the integer number of resets at time t:

$$Q_{out}(t) = Q_o * N(t) \tag{2.4}$$

eq:qout)

Where Q_o is the fixed amount of charge discharged during each reset. Equation **??** then can give us the maximum current output using the definition of current $I = \frac{dQ}{dt}$, then

$$I_{max} = \frac{d}{dt}(Q_o * N(t)) = Q_o \frac{dN}{dt} = Q_o * f \tag{2.5}$$

eq:imax)

Where we identify that the maximum value of $\frac{dN}{dt} = f$, with f as the clock frequency of the local digital block. Equation **??** relates the maximum current to the digital clock frequency and the amount of charge discharged during each reset. Then we take the nominal expected frequency , charge, and voltage values to calculate an expected I_{max}:

$$I_{max} \approx 1\ fF * 1\ V * 30 * 10^6 MHz \approx 30\ nA \tag{2.6}$$

We note that 30 nA is much greater than the expected background current from Ar^{39} ($\mathcal{O}(10^{-18})A$). However, the more interesting events deposit more more charge, and we can use the average drift speed of electrons in a LArTPC to estimate the maximum charge density we can be sensitive to:

$$\lambda_{max} = \frac{dQ}{dL} = \frac{dQ}{dt} / \frac{dx}{dt} = \frac{I_{max}}{v_{drift}} \tag{2.7}$$

We use a nominal v_{drift} speed of 1.6mm / μs, and convert to SI units to obtain λ_{max} in equation 2.1:

$$\lambda_{max} = \frac{3 * 10^{-8} A}{1600 \frac{m}{s}} = 1.875 * 10^{-11} \frac{C}{m} \approx 19 \frac{nC}{mm} \tag{2.8}$$

We can now use this result to calculate a maximum $\frac{dE}{dx}$ measurement:

$$\frac{dE}{dx}_{max} = \frac{dQ}{dx}_{max} \frac{dE}{dQ} = \lambda_{max} \frac{dE}{dQ} \tag{2.9}$$

We can take the ionization energy of Ar^{39} to be $\approx 23.6keV$, then:

$$1electron = 23.6keV$$

and

$$1electron = 1.602 * 10^{-19} C$$

Then $\frac{dE}{dQ}$ becomes:

$$\frac{dE}{dQ} = \frac{23.6keV}{1.602 * 10^{-19} C} \tag{2.10}$$

Finally, we calculate the result of equation **??** and convert to units of $\frac{GeV}{mm}$.

$$\frac{dE}{dx}_{max} = 1.875 * 10^{-11} \frac{C}{m} * \frac{23.6keV}{1.602 * 10^{-19} C} \approx 2.76 \frac{GeV}{mm} \tag{2.11}$$

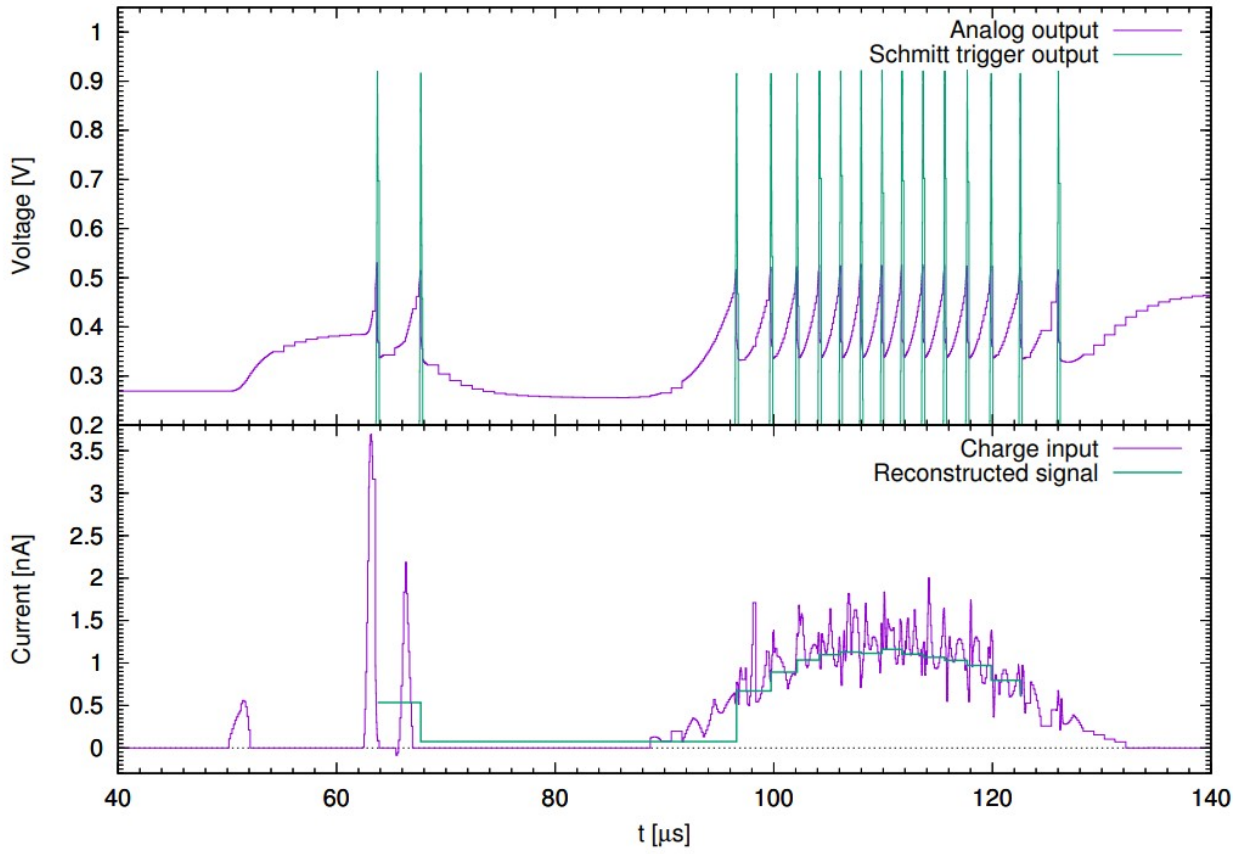

Figure 2.2: Example reconstruction of the reset time difference (RTD) based on the Q-Pix readout design. Image is taken from [3].

Background Calibration

Calibration measurements are essential for any detector. Here we describe an automatic use of existing Ar^{39} decays as a source of calibration at the pixel level.

The value which needs to be calibrated is the pixel's response to an input charge Q_{in} in equation 2.1. Given some stable input charge, there should be a known number of reset measurements to calibrate against.

The capacitance (C_i) for each pixel is a systematic which can be calibrated periodically using the background current from Ar^{39} decay.

Once the trigger voltage (V_i) is exceeded the schmidt trigger issues the timing reset which is then

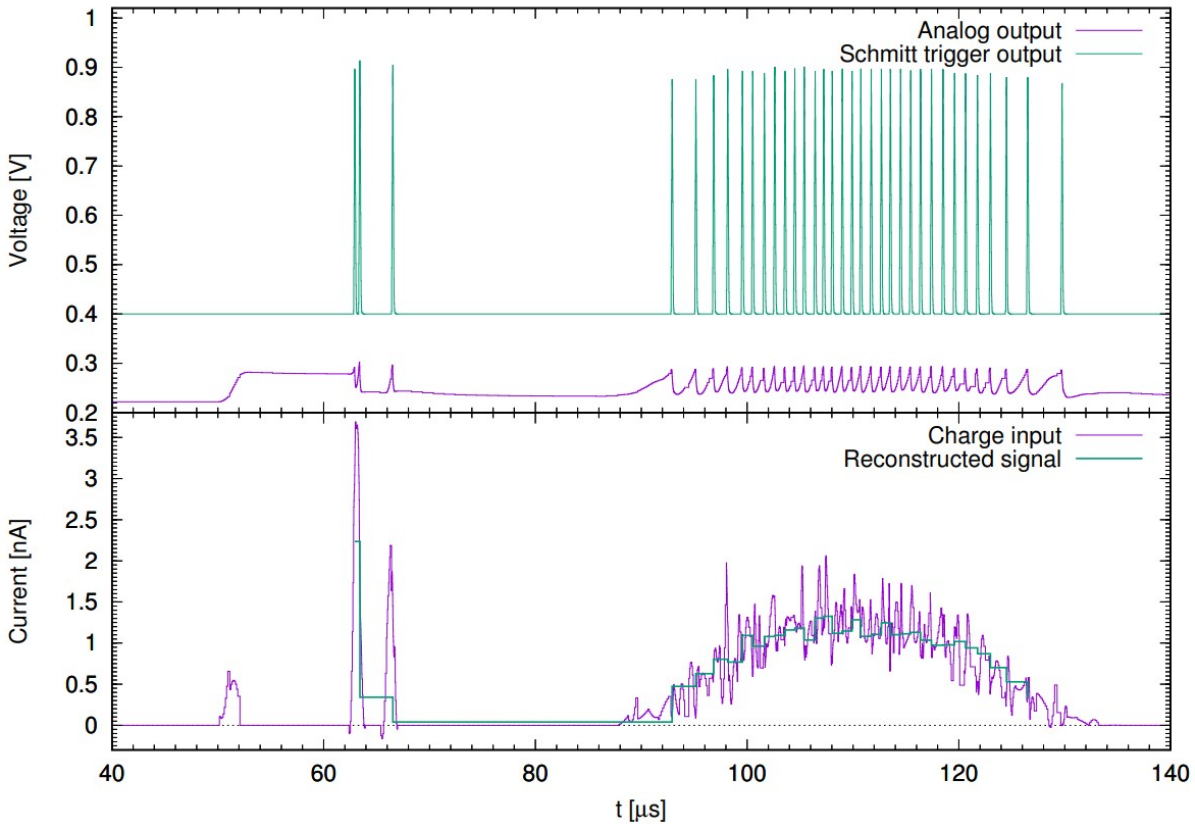

Figure 2.3: Example reconstruction of the reset time difference (RTD) based on the Q-Pix readout design. delta-Q was chosen to be $0.3fC$. Image is taken from [3].

recorded as a 32-bit digital timestamp. This timestamp value is recorded against a free running local oscillator ($\approx$ 30 MHz). The number of free running clocks in the entire system is expected to be the number of channels (N_c) divided by the number of digitally multiplexed channels (N_d), which are taken to be 16.

Making a 3-D Image

One of the important features of a TPC is the ability to reconstruct full 3-D images. The intended benefit of a pixelated readout on any TPC is to show that there are improvements to reconstruction of these 3-D images.

In order to reconstruct the image of the interaction from a set of data above the pixel the required data are the reset time at a pixel i (T_{ri}), event time (T_e), and the pixel ID. We assume that T_e (as is normally used to tag events in TPCs) uses a trigger time from a secondary PMT system from

the scintillation light produced by the interaction to tag an event of interest. Since the scintillation photons travel much faster than the drift electrons, we can use the T_e as the starting time.

The pixel ID of each reset gives two of the three remaining coordinates ($\hat{x}$ and $\hat{y}$). The last coordinate ($\hat{z}$) is reconstructed using T_{ri}.

Since the drift velocity of the electrons (v_e) is constant in a TPC the distance that the electrons traveled to reach the anode plane ($\hat{z}$) is determined based on only the drift time:

$$z = v_e * T_{drift} \tag{2.12}$$

However, this drift time is measured directly from the difference between the event time (T_e) and the reset time for this pixel (T_{ri}).

$$T_{drift} = T_{ri} - T_e \tag{2.13}$$

The drift distance in equation (2.1) becomes:

$$z = v_e * (T_{ri} - T_e) \tag{2.14}$$

Uncertainties

Therefore the precision of the measurement of $\hat{z}$ is based on equation 2.1. The uncertainty for the two transverse coordinates on the anode plane ($\hat{x}$ and $\hat{y}$) which are reasonable assumed to be uniform over the pixel are then $\frac{3mm}{\sqrt{12}} \approx 0.87mm$.

Bad Scenarios

Here we briefly describe potential issues of the readout circuit presented here.

Maximum Reset Rate

2.2 System Requirements

This differs from other concepts such as Genetic Multiplexing ([32]) and using only regions of interest (ROI).

Therefore, the total number of free running oscillators (N_{osc}) per DUNE-APA for a given pixel pixel of 3 mm^2 is:

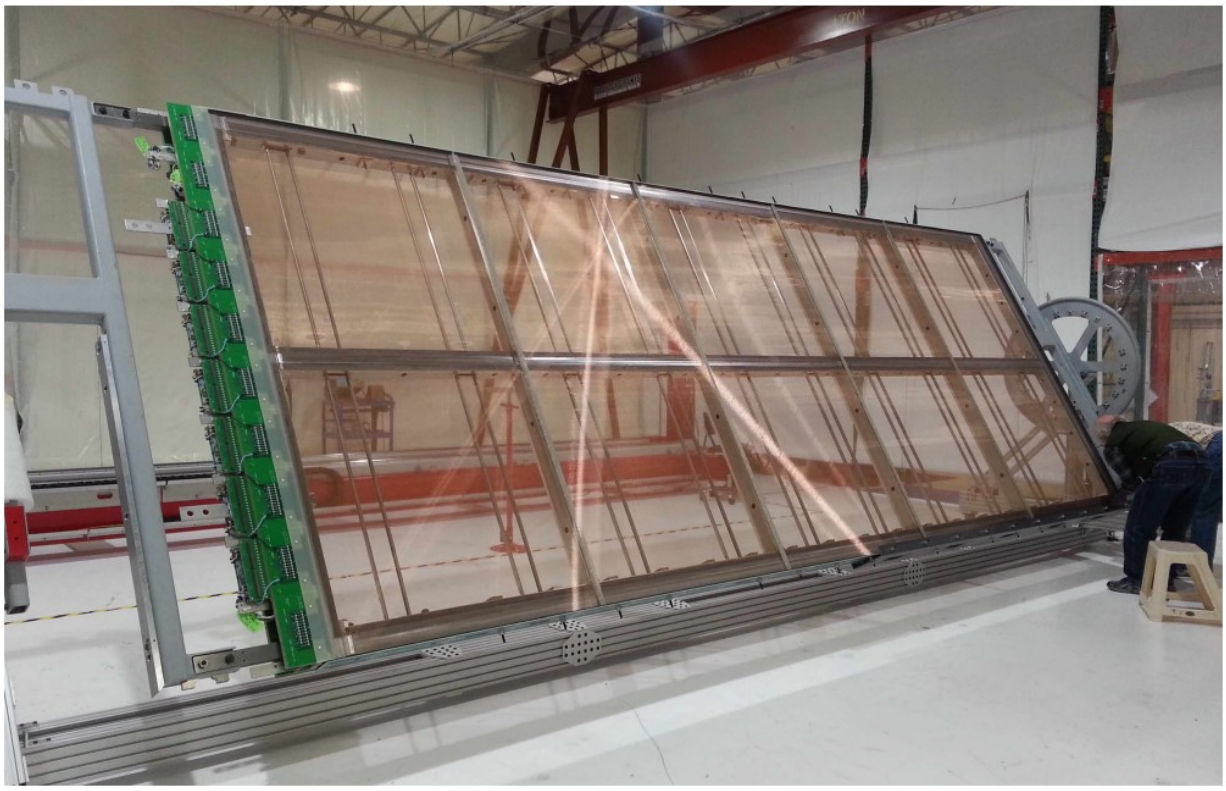

Figure 2.4: A simple caption [4]

$$N_{osc} = \frac{6.3 * 2.5}{9 * 10^{-6} * 16} = 109375 \tag{2.15}$$

Therefore we expect the order of the number of free running oscillators per DUNE-APA $O(10^5)$.

Single Point Failures

2.3 How Q-Pix fits into a DUNE APA

DUNE Anode Plane Assemblies (APA) designs are based on [4].

Chapter 3

NEW DIFFUSION MEASUREMENTS: STUDIES WITHIN SAQ

In this chapter we introduce the first implementation of the Q-Pix based design using purely "over-the-counter" electronics.

3.1 Simplified Analog Q-Pix: System Design

3.2 Leakage Current Measurements

3.3 TPC Design

3.4 Diffusion in Noble Gasses

Measurements of Transverse and Longitudinal diffusion of electrons within electric fields of strength 500 V/cm have been performed before [33].

3.5 Measurements of Drift Current

3.6 LArTPC Diffusion background

3.7 Xenon Gas Lamp Measurements

Integrating towards background Current

3.8 Results

Chapter 4

THE DIGITAL BACK-END AND VIABILITY STUDIES

In this chapter we describe the overall structure digital back-end of the Q-Pix design. We would like to take a moment here to note here that we refer to each node in the array is implemented as a lattice ice40UP FPGA

Additionally, this chapter is divided into two parts. The first part we give a detailed description of the digital-system, and its requirements to successful in a Q-Pix based detector of DUNE scales. The motivation here is to outline how the digital backend of Q-Pix based readout fits into the DUNE-FD LArTPC. The second part of this chapter is dedicated to the first evaluation boards developed and tested which are implemented in Lattice iCE40UP FGPAs [34]. The second part outlines the design of the PCB on which these FPGAs are implemented, as well as basic results of these FGPAs, which are motivated from the first part of this chapter.

The Lattice Semiconductor FPGAs [34] were selected because of the small form factor, pin out, availability, as well as lower power consumption. There are planned tests for future, but not presented here to indicate its viability of over-the-counter FPGAs in LArTPc. If such cheap and available FPGAs were shown to be reliable use in a LArTPC environment, that would greatly influence future detector development and selection for Q-Pix.

4.1 Digital Design Overview

The digital system of the entire Q-Pix design begins at the electronic collection of a recorded timestamp in respond to a reset-time-difference sent from the analog front-end. Then, all data that are recorded for each pixel, and the only data required for a full analysis of all reconstruction with a LArTPC are:

- 32 bit timestamp
- Pixel X location ($\leq$ 4 bits)
- Pixel Y location ($\leq$ 4 bits)
- APA reference number ($\leq$ 4 bits)

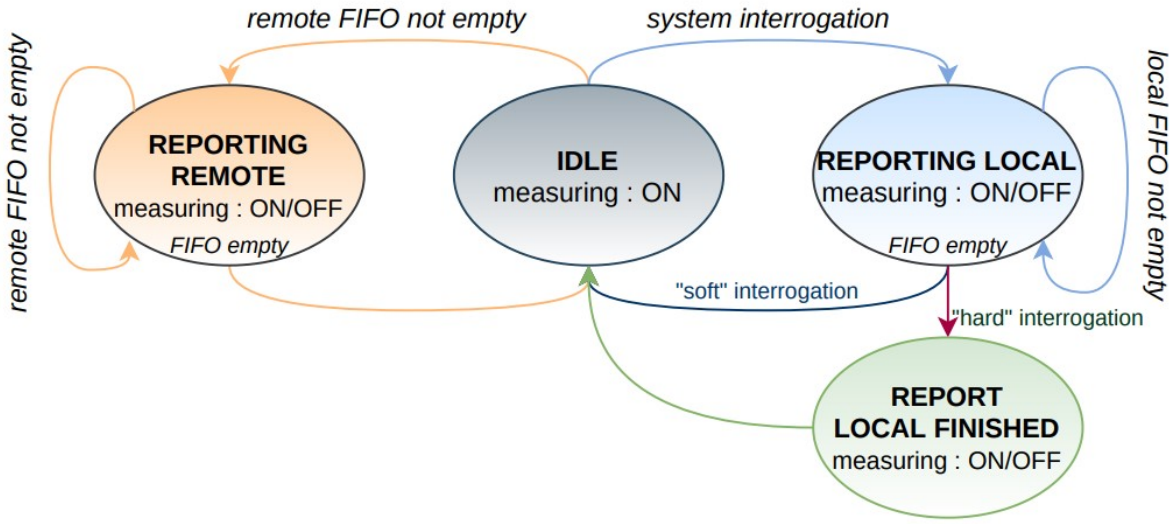

Figure 4.1: Diagram of the Digital node's FSM which determines how to respond to incoming packets.

Each of these remote ASICs are running on free-running independent clocks, with an expected frequency of $\approx$ 30 MHz.

Basic System Requirements

Reset time differences are a function of the accumulated charge compared to the integrating capacitance for this specific pixel. The sheer number of pixels required for an APA (and the entire module) require an effective means of charge and time calibration, stable buffer depths, and protection against single-point failure (SPF).

Charge Calibration of each Pixel

Natural decay products produced by $^{3}9$Ar provide a continous source of incoming current across a LArTPC.

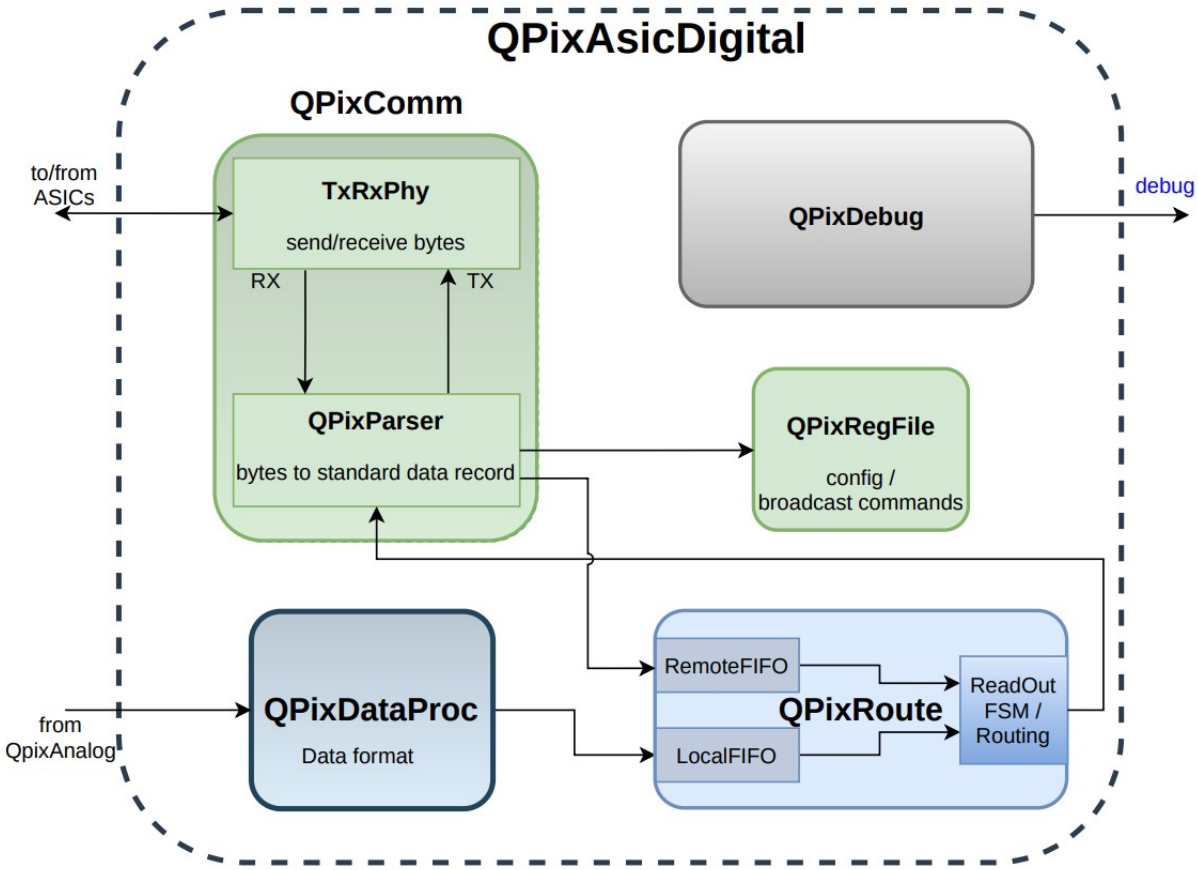

Figure 4.2: Diagram of the Digital node.

Time Calibration of each Node

Inter-Node communication via endeavor protocol

The Structure of a Data Word

Each node communicates via an entire packet, which is always 64 bits long. The communication protocol (4.1)

Comments on Data Rates and required Computing

Based on the minimum number of bits for each RTD 4.1 we can calculate minimum data rates for a full APA section and extend to this to

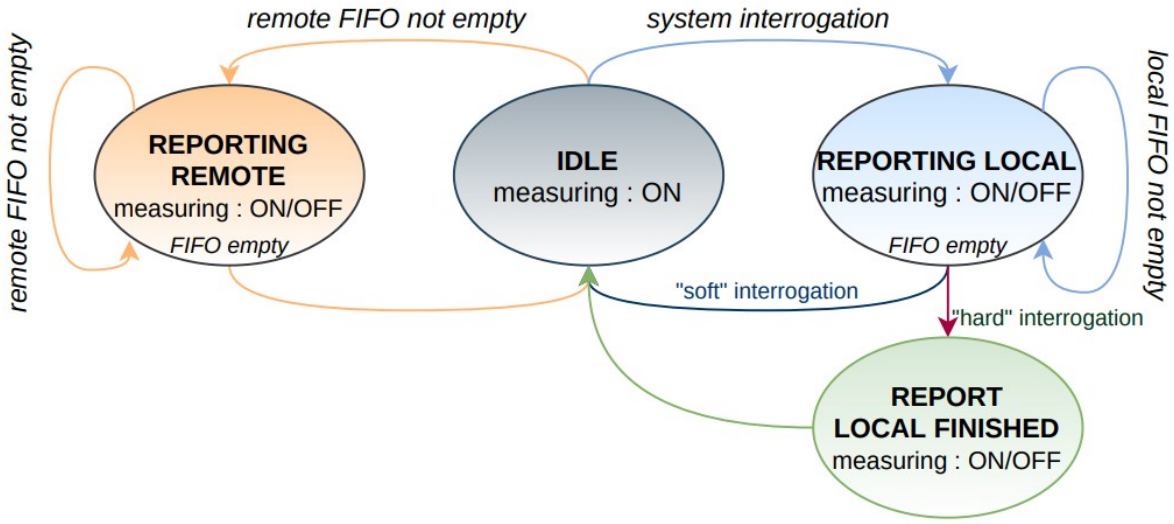

Figure 4.3: Overview of the FSM design, courtesy of Vasily Shebalin.

4.2 The Digital Finite State Machine

The Finite State Machine (FSM) of the remote digital ASIC outlines the designed behavior response to inputs from a controlling DAQ node.

- Idle, Acquisition State
- Transmit Local
- Transmit Finish
- Transmit Remote
- DONE

4.3 The Parameter Space of the Digital System

Buffer Depth Requirements

The required buffer depth of each node in an array is the maximum number of timestamps the node can store in memory before running out of room.

4.4 QDB Design Overview

4.5 Power and Current Characteristics

4.6 Timing Stability

We describe here the methods of measuring a stable time for different configurations of the nodes. We also comment on the results of the timing with resepect to the minimum required timing sensitivity in order to have accurate timestamp reconstruction.

4.7 Analysis of Systematics for Different System Implementations

4.8 Towards the Integration of a DAQ-Node

4.9 Comments on A Super-DAQ-Node

Each APA module within a larger DUNE module must ultimately be interconnected so that the entire module can be readout. As described above, a single modular tile is controlled by an individual DAQ node, where many constitute a complete APA. Therefore, we refer to the device that digitally multiplexes all of the DAQ node data as the "Super DAQ Node" (SDN). Then, we imagine the final multiplexing stage for an entire DUNE module as an array of SDNs, each of which consistute an array of DAQ nodes, where each DAQ node is a 2-D array of Q-Pix based ASICs.

The total number of request SDNs within the full dune module depends on the final size of a DAQ-node controlled tile.

4.10 Summary

Chapter 5

SIMULATION STUDIES AND FUTURE Q-PIX PROTOTYPES

5.1 Physical Simulation Studies

5.2 Background Rates and Calibration

sources of backgrounds are taken from [4]

5.3 Supernova Studies

Work has been done to understand how a Q-Pix based DUNE-FD would measure core collapse supernovae [35].

Simulation studies which involved particle interactions were based on Geant4 [36].

5.4 Looking for Hadron Decay

5.5 Neutrino Beam High Energy Studies

5.6 Further Studies

Chapter 6

SUMMARY AND OUTLOOK

Recap of Qpix Requirements for DUNE APA here.

Recap of Qpix design concept testing within SAQ here.

Recap of QDB Results here

Recap of SAQ Results here

Recap of lessons learned on pixelated detectors

Discuss how combination of simulation / qdb / saq results motivate the next stage of development for QPix and incorporating the digital / analog ASICs for round two.

BIBLIOGRAPHY

[1]D. Dominguez, *Cern accelerating science*, 2015.

[2]R. Acciarri et al., *Long-baseline neutrino facility (lbnf) and deep underground neutrino experiment (dune) conceptual design report volume 1: the lbnf and dune projects*, 2016.

[3]D. Nygren and Y. Mei, *Q-pix: pixel-scale signal capture for kiloton liquid argon tpc detectors: time-to-charge waveform capture, local clocks, dynamic networks*, 2018.

[4]B. Abi et al., "Volume iv. the dune far detector single-phase technology", Journal of Instrumentation **15**, T08010 (2020).

[5]J. L. Hewett et al., *Fundamental physics at the intensity frontier*, 2012.

[6]"Juno physics and detector", Progress in Particle and Nuclear Physics **123**, 103927 (2022).

[7]D. A. Glaser, "Some effects of ionizing radiation on the formation of bubbles in liquids", Phys. Rev. **87**, 665–665 (1952).

[8]J. Chadwick, "The intensity distribution in the magnetic spectrum of beta particles from radium (B + C)", Verh. Phys. Gesell. **16**, 383–391 (1914).

[9]J. S. Chadwick, "Possible existence of a neutron", Nature **129**, 312–312 (1932).

[10]E. Fermi, "Versuch einer Theorie der β-Strahlen. I", Zeitschrift fur Physik **88**, 161–177 (1934).

[11]C. L. Cowan, F. Reines, F. B. Harrison, H. W. Kruse, and A. D. McGuire, "Detection of the free neutrino: a confirmation", Science **124**, 103–104 (1956).

[12]K. Abe et al. (T2K Collaboration), "Measurements of neutrino oscillation in appearance and disappearance channels by the t2k experiment with 6.6×10^{20} protons on target", Phys. Rev. D **91**, 072010 (2015).

[13]F. P. An et al., "Observation of electron-antineutrino disappearance at daya bay", Phys. Rev. Lett. **108**, 171803 (2012).

[14]G. Charpak, R. Bouclier, T. Bressani, J. Favier, and C. Zupancic, "The Use of Multiwire Proportional Counters to Select and Localize Charged Particles", Nucl. Instrum. Meth. **62**, 262–268 (1968).

[15]J. N. Marx and D. R. Nygren, "The time projection chamber", Physics Today **31**, 46–53 (1978).

[16]C. Rubbia, *The liquid-argon time projection chamber: a new concept for neutrino detectors*, tech. rep. (1977).

[17]R. Acciarri et al. (ArgoNeuT Collaboration), "Demonstration of mev-scale physics in liquid argon time projection chambers using argoneut", Phys. Rev. D **99**, 012002 (2019).

[18]R. Acciarri et al., "Design and construction of the microboone detector", Journal of Instrumentation **12**, P02017 (2017).

[19]R. Acciarri et al., "The liquid argon in a testbeam (lariat) experiment", Journal of Instrumentation **15**, P04026 (2020).

[20]A. Friedland and S. W. Li, "Understanding the energy resolution of liquid argon neutrino detectors", Phys. Rev. D **99**, 036009 (2019).

[21]B. Abi et al., "Volume i. introduction to dune", Journal of Instrumentation **15**, T08008 (2020).

[22]B. Abi et al., *Deep underground neutrino experiment (dune), far detector technical design report, volume ii: dune physics*, 2020.

[23]B. Abi et al., "Volume iii. dune far detector technical coordination", Journal of Instrumentation **15**, T08009 (2020).

[24]L. Paulucci and on behalf of DUNE collaboration, "The dune vertical drift photon detection system", Journal of Instrumentation **17**, C01067 (2022).

[25]F. Arneodo, *The icarus experiment, a second-generation proton decay experiment and neutrino observatory at the gran sasso laboratory*, 2001.

[26]P. Sadowski, B. Radics, Ananya, Y. Yamazaki, and P. Baldi, "Efficient antihydrogen detection in antimatter physics by deep learning", Journal of Physics Communications **1**, 025001 (2017).

[27]P. Sadowski and P. Baldi, "Deep learning in the natural sciences: applications to physics", in Braverman readings in machine learning (2017).

[28]D. Dwyer, M. Garcia-Sciveres, D. Gnani, C. Grace, S. Kohn, M. Kramer, A. Krieger, C. Lin, K. Luk, P. Madigan, C. Marshall, H. Steiner, and T. Stezelberger, "Larpix: demonstration of low-power 3d pixelated charge readout for liquid argon time projection chambers", Journal of Instrumentation **13**, P10007 (2018).

[29]J. Asaadi, M. Auger, A. Ereditato, D. Goeldi, R. Hänni, U. Kose, I. Kreslo, D. Lorca, M. Luethi, C. R. von Rohr, J. Sinclair, F. Stocker, C. Tognina, and M. Weber, "A pixelated charge readout for liquid argon time projection chambers", Journal of Instrumentation **13**, C02008 (2018).

[30]F. Sutanto, T. Classen, S. Dazeley, M. Duvall, I. Jovanovic, V. Li, A. Mabe, E. Reedy, and T. Wu, "Sandd: a directional antineutrino detector with segmented 6li-doped pulse-shape-sensitive plastic scintillator", Nuclear Instruments and Methods in Physics Research Section A: Accelerators, Spectrometers, Detectors and Associated Equipment **1006**, 165409 (2021).

[31]J. Joshi and X. Qian, *Signal processing in the microboone lartpc*, 2015.

[32]S. Procureur, R. Dupré, and S. Aune, "Genetic multiplexing and first results with a 50×50cm2 micromegas", Nuclear Instruments and Methods in Physics Research Section A: Accelerators, Spectrometers, Detectors and Associated Equipment **729**, 888–894 (2013).

[33]Y. Li, T. Tsang, C. Thorn, X. Qian, M. Diwan, J. Joshi, S. Kettell, W. Morse, T. Rao, J. Stewart, W. Tang, and B. Viren, "Measurement of longitudinal electron diffusion in liquid argon", Nuclear Instruments and Methods in Physics Research Section A: Accelerators, Spectrometers, Detectors and Associated Equipment **816**, 160–170 (2016).

[34]Lattice, *Ice40 ultraplus family data sheet*, lattice ice40up fpga data sheet, Lattice Semiconductor (https://www.latticesemi.com/-/media/LatticeSemi/Documents/DataSheets/iCE/iCE40-UltraPlus-Family-Data-Sheet.ashx).

[35]S. Kubota et al. (Q-Pix Collaboration), "Enhanced low-energy supernova burst detection in large liquid argon time projection chambers enabled by q-pix", Phys. Rev. D **106**, 032011 (2022).

[36]S. Agostinelli et al., "Geant4—a simulation toolkit", Nuclear Instruments and Methods in Physics Research Section A: Accelerators, Spectrometers, Detectors and Associated Equipment **506**, 250–303 (2003).

[37]A. Galindo-Tellez, K. Keefe, E. Adamek, E. Brubaker, B. Crow, R. Dorrill, A. Druetzler, C. J. Felix, N. Kaneshige, J. G. Learned, J. J. Manfredi, K. Nishimura, B. Pinto Souza, D. Schoen, and M. Sweany, "Design and calibration of an optically segmented single volume scatter camera for neutron imaging", Journal of Instrumentation **16**, P04013, P04013 (2021).

Appendix A

SVSC OS1

the work in this subsection details the work and results of [37].

Appendix B

SVSC OS2

The section lists the work detailed in [**svsc_os2_Keefe_2022**].